Analyst

PAPER

View Article Online
View Journal

Cite this: DOI: 10.1039/c6an00626d

Sensitive fluorescence assay of organophosphorus pesticides based on the fluorescence resonance energy transfer between CdTe quantum dots and porphyrin†

Gao Xue, Zhao Yue, Zhang Bing, Tang Yiwei, Liu Xiuying and Li Jianrong*

Received 16th March 2016,
Accepted 3rd June 2016

DOI: 10.1039/c6an00626d

www.rsc.org/analyst

A sensitive and selective quantum dot (QD)-based fluorescence resonance energy transfer (FRET) biosensor was successfully fabricated for the detection of organophosphorus pesticides (OPs). 5,10,15,20-Tetra(4-pyridyl)porphyrin (TPyP) with *meso*-pyridyl substituents was bound to the surface of CdTe QDs to produce self-assembled nanosensors, and the process of FRET between QDs and TPyP occurred. However, the process of FRET was switched off with the addition of OPs, due to the combination between TPyP and OPs. The fluorescence intensity of TPyP (donor) would decrease gradually with the increasing concentration of OPs. Under optimal conditions, a linear correlation was established between the fluorescence intensity ratio I_{TPyP}/I_{QDs} and the concentration of paraoxon in the range of 9.09×10^{-12}–1.09×10^{-6} mol L^{-1} with a detection limit of 3.15×10^{-12} mol L^{-1}. The attractive sensitivity was obtained due to the efficient FRET and the superior fluorescence properties of QDs. The proposed method was successfully applied to the determination of the OPs in real fruit samples with satisfactory results.

Introduction

Organophosphate pesticides (OPs) exposure is a growing global health problem, posing a highly severe threat to human life. OPs are found to be quite toxic and their acute toxicity can be ascribed to their irreversible phosphorylation and inactivation of acetylcholinesterase, an essential enzyme involved in the cholinergic functions, in the central and peripheral nervous system. Consequently, OPs inhibit the hydrolysis of the neurotransmitter acetylcholine, resulting in the *in vivo* accretion of acetylcholine, which inflicts various clinical complications including respiratory tract paralysis or even death.[1] Well-established detection methods for OPs such as classical gas chromatography (GC) and high-performance liquid chromatography (HPLC) offer high sensitivity and selectivity for accurate determination of OPs.[2–4] Nevertheless, they require complex and expensive instrumentation and centralized laboratories. Various analytical devices such as fluorescent probes,[5] electrochemical sensors,[6] immunosensors[7] and fluorescent resonance energy transfer (FRET)–quantum dot (QD) based sensors[8,9] have been developed to overcome these challenges in the past decade.

FRET is a non-radiative process whereby a donor in an excited state transfers energy to an acceptor in a proximal ground state, resulting in an increase in the energy level of the latter. Generally, an effective FRET process could only occur, when the emission spectrum of the donor and the absorption spectrum of the acceptor overlap appreciably and the mutual distance of the donor–acceptor pair is near enough (1–10 nm). Until now, because of the specificity and the intrinsic sensitivity of FRET to small changes in the donor–acceptor distance, it has been utilized in various research areas, especially in analytical and bioanalytical chemistry.[10] Recently, QDs have been widely employed as donors in FRET-based systems for signaling probes due to several distinguished properties over common organic fluorescent dyes, which include high quantum yields, broad absorption spectra coupled to narrow size-dependent emissions and exceptional resistance to photobleaching.[11–13] Furthermore, QD emission wavelengths can cover a wide range from the visible to near-infrared regions, and can therefore easily overlap with the absorption spectrum of an acceptor at certain wavelengths, leading to the possibility of FRET between the QDs and the acceptor.

Porphyrin is a macrocyclic molecule with unique photophysical and electrochemical properties. The optoelectronic properties of porphyrins were tuned by varying the *meso*-

College of Chemistry, Chemical Engineering and Food Safety, Bohai University, Jinzhou 121013, People's Republic of China. E-mail: huaxue_gaoxue@126.com, lijr6491@163.com; Tel: +86-416-3400151

†Electronic supplementary information (ESI) available. See DOI: 10.1039/c6an00626d

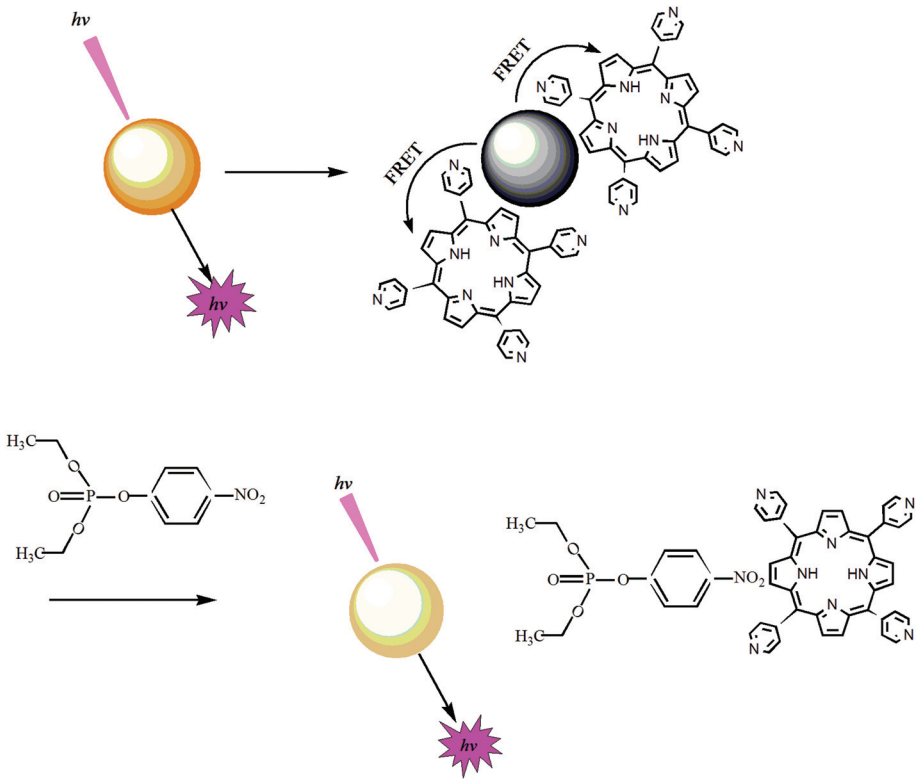

Scheme 1 Proposed fluorescence resonance energy transfer mechanism based on a QD/TPyP complex for paraoxon assay.

functional ligands and metal insertion sites.[14] Porphyrins have been used in a wide range of sensor applications. The sensitivity of the porphyrin spectrum makes porphyrins ideal for use as indicators in absorbance or fluorescence spectroscopy.[15] The representative porphyrins have the great ability to interact not only with the DNA chain and its particular elements,[16–19] but also with different kinds of biologically active compounds, like paraoxon[20] and toxic metal ions.[21] Porphyrin compounds are widely employed as a platform to recognize various species because of their structures with highly delocalized π-bonds and the unique properties of the tetraphenylporphyrin core which has the ability to participate in hydrogen bonding with the anion to form the hydrogen bond donor–acceptor complexes.[22] With the great progress made in nanoscience and nanotechnology, interest has been increasing in exploring the orderly assembly of porphyrin with various nanostructures including semiconductor TiO_2, CdSe QDs and carbon nanotubes (CNTs). Recently, Patra *et al.* utilized the QD–porphyrin systems as optical-based sensors for bio applications.[23] Borczyskowski *et al.* have widely analyzed the photophysical properties of QDs with porphyrin systems.[24]

In this paper, a novel FRET biosensor, with CdTe QDs and porphyrin as the energy donor–acceptor pairs, is developed for OP detection. The fluorescence quenching of CdTe QDs in the presence of porphyrin indicates the efficient energy transfer from QDs to porphyrin. In OP medium, OPs act as a receptor to bind the porphyrin and the fluorescence intensity of porphyrin would decrease by preventing the energy transfer from QDs to porphyrin, as illustrated in Scheme 1. The OP assay can thus be accomplished by the QD/TPyP probe operating with a novel FRET model. Also, the selectivity and sensitivity of the sensor system based on FRET were proved with real sample tests. The novel system, which could detect paraoxon in low detection limits, was developed.

Experimental section

Materials and apparatus

All chemicals were of analytical reagent grade and used without further purification. Mercaptopropionic acid (MPA) (99%), tellurium powder (~200 mesh, 99.8%), $CdCl_2$ (99%), $NaBH_4$ (99%), and 5,10,15,20-tetra(4-pyridyl)porphyrin (TPyP) were purchased from Sigma–Aldrich. Paraoxon standard reagent (1000 μg mL^{-1}, acetone solution) was purchased from Shenzhen Shidejia Biotechnology Company. The water used in all experiments had a resistivity higher than 18 MΩ cm^{-1}. Fluorescence measurements were performed on a FluoroMax-4 fluorophotometer (HORIBA Jobin Yvon, NJ, USA), and 1 cm path-length quartz cuvettes were used in experiments. All pH measurements were carried out with a PHS-3C pH meter (Tuopu Co., Hangzhou, China).

Preparation of CdTe QDs

Water compatible CdTe QDs used in this study were synthesized by refluxing routes with mercaptopropionic acid

(MPA) as a stabilizer.[25] Briefly, sodium hydrogen telluride (NaHTe) was produced in aqueous solution by the reaction of sodium borohydride ($NaBH_4$) with tellurium powder in a molar ratio of 2 : 1. Later, fresh NaHTe solution was added to 10 mmol L^{-1} $CdCl_2$ solutions at pH 11.2 in the presence of MPA with N_2 protection, and the molar ratio of Cd^{2+}/MPA/HTe^- was fixed at 1 : 2.4 : 0.2. The CdTe precursor solution was subjected to a reflux at 100 °C under open-air conditions with a condenser attached. The stable water-compatible CdTe QDs showed emission peaks at 610 nm upon excitation at 400 nm. According to the calculation method in Wang *et al.* (2008),[25] the concentration of CdTe QDs is 2.0×10^{-6} mol L^{-1}.

General procedures for fluorescence detection of paraoxon

A typical FRET-based analysis of paraoxon was performed as follows. 200 μL CdTe QD solution (2.0×10^{-7} mol L^{-1}) was added to different concentrations of TPyP solution. The mixture was diluted to 1.5 mL with PBS (10.0 mmol L^{-1}, pH 8.5), and the fluorescence spectra were recorded immediately. 200 μL CdTe QD solution (2.0×10^{-7} mol L^{-1}) and 200 μL TPyP solution (1.0×10^{-5} mol L^{-1}) were added into 2 mL centrifuge tubes with different concentrations of paraoxon. The mixture was diluted to 1.5 mL with PBS (10.0 mmol L^{-1}, pH 8.5) and incubated at room temperature for 15 min. Afterwards, the fluorescence emission spectra were recorded with an excitation of 400 nm. The calibration curve for paraoxon was established according to the fluorescence enhancement efficiency, which was monitored by I_{TPyP}/I_{QDs} (where I_{TPyP} and I_{QDs} refer to the fluorescence intensity of TPyP and CdTe QDs, respectively).

Procedures for paraoxon sensing in apple samples

In the present work, the fruit samples were simply pretreated without using organic solvents and tedious preconcentration steps. Further experiments were performed with the intentional addition of paraoxon onto the apple surface. Paraoxon in apple samples was measured to evaluate the potential of this assay for pesticide screening in real-world applications. The apple samples were pretreated according to the method of GB/T5009.199-2003.[26] 1 g of apple samples was weighed and finely chopped to 1 cm^3, then dissolved in 5 mL purified water and ultrasonicated for 2 min. After allowing it to stand for 3–5 min, different concentrations of paraoxon standard solutions were added into the obtained matrix of apple samples. The supernatant was collected for analysis according to the method in the preceding section. For recovery experiments, known quantities of paraoxon were injected into the finely chopped apples, then pretreated and analyzed according to the above procedures.

Results and discussion

Optical characteristics of CdTe QDs and TPyP

The absorption and emission spectra of the two separate components, CdTe QDs and TPyP, are given in Fig. 1. As shown in Fig. 1, the fluorescence emission of QDs and the absorption spectrum of TPyP had a remarkable spectral overlap, indicating the potential to produce efficient energy transfer from QDs (as a donor) to TPyP (as an acceptor). By contrast energy transfer from TPyP to QDs is unlikely, because of both the energy disparity and the lack of overlap between the QD absorption and TPyP emission. The FRET detection was performed by exciting the donors at 400 nm in order to make the contribution of the fluorescence of the acceptor coming from direct excitation of the acceptor as little as possible.

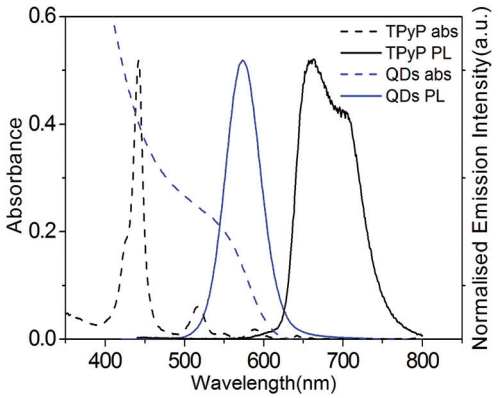

Fig. 1 Normalized absorption and fluorescence spectra of CdTe QDs and TPyP solution.

FRET-based nanoscale assemblies of CdTe QDs and TPyP

Before we discussed the CdTe QD–TPyP system, it was important to know how QDs and TPyP were attached to each other. Upon mixing the dilute aqueous solutions of QDs with TPyP, the complexes were formed by the electrostatic association of TPyP on the surface of MPA-capped CdTe QDs. Actually, MPA-capped QDs are negatively charged (due to the presence of carboxylate groups on the surface) and TPyP molecules are positively charged (due to the acidification by H_2SO_4). Therefore, the negatively charged CdTe QDs and the positively charged TPyP molecules are in close proximity due to electrostatic interaction. It can be seen from Fig. 2 that the fluorescence intensity of CdTe

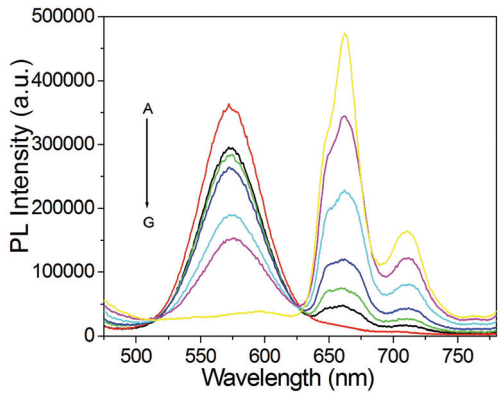

Fig. 2 The fluorescence spectra of the FRET system with different concentrations of TPyP, A–G: 0, 3.33×10^{-7}, 6.67×10^{-7}, 1.33×10^{-6}, 2.67×10^{-6}, 4.0×10^{-6} and 5.33×10^{-6} mol L^{-1}, respectively.

QDs gradually decreased and the fluorescence intensity of TPyP increased along with the increasing concentrations of TPyP. The quenching of QD luminescence *via* energy transfer was examined as a function of the disposition of pyridyl rings at the *meso* positions. It has been reported that two *cis*-pyridyl rings facilitate porphyrin binding to the QD surface to form a QD/porphyrin conjugate.[27] The enhancement of porphyrin emission upon association of the QDs is a result of FRET. In these assemblies, the QDs serve as the antenna for photon absorption. Energy is passed from the QD donor to the porphyrin acceptor by the FRET mechanism as illustrated in Scheme 1.

In almost all the chemistry experiments related to FRET, the energy transfer efficiency (E) will have to be calculated in order to get a relative accurate value for the efficiency of energy transfer.[28,29] E can be measured and calculated according to the following equation:

$$E = 1 - I/I_0 \quad (1)$$

where I refers to the fluorescence intensity of the donors (CdTe QDs) in the presence of the acceptor (porphyrin) and I_0 refers to the fluorescence intensity of the donor in the absence of the acceptor.

The relationship between the energy transfer efficiency and the distance between the donor–acceptor pair is expressed as

$$E = {R_0}^6/({R_0}^6 + R^6) \quad (2)$$

where R is the real distance between the donor–acceptor pair and R_0 is the critical distance between the donor–acceptor pair at 50% energy transfer efficiency, which is calculated using the following equation:

$${R_0}^6 = 8.8 \times 10^{-25}\ K^2 n^{-4} \Phi J(\lambda) \quad (3)$$

where K^2 refers to the spatial orientation factor with the value of 2/3. n refers to the refractive index with the value of 1.336. Φ refers to the quantum yield of CdTe QDs in our experiments, which can be measured using rhodamine 6G as the reference standard, with the value of 47%. $J(\lambda)$ refers to the spectral overlap integral, which can be calculated from the following equation:

$$J(\lambda) = \left[\sum I(\lambda)\varepsilon(\lambda)\ \lambda^4 \Delta\lambda\right] / \left[\sum I(\lambda)\ \Delta\lambda\right] \quad (4)$$

where $I(\lambda)$ is the fluorescence intensity of the fluorescence donor at the wavelength λ, $\varepsilon(\lambda)$ is the molar absorption coefficient of the acceptor at wavelength λ and its unit is L mol^{-1} cm^{-1}. The overlap between the absorption spectrum of CdTe QDs and the fluorescence emission spectrum of porphyrin is shown in Fig. 1. $J(\lambda)$ could therefore be calculated by eqn (4) from the spectrum of FRET for λ = 420–780 nm, and the value of $J(\lambda)$ is 1.696×10^{-13} cm^3 L mol^{-1}. The R_0 is calculated to be 3.85 nm according to eqn (3).

In this study, the energy transfer efficiency (E) could reach 90.0% according to eqn (1), and the distance between the QDs and porphyrin was 2.63 nm according to eqn (2), which was small enough to make the FRET occur, indicating that the energy transfer from CdTe QDs to porphyrin occurred with high probability.

Effects of paraoxon on the optical characteristics of TPyP

As discussed above, CdTe QDs and TPyP can form FRET donor–acceptor assemblies, resulting in effective quenching of QD emission, while QD–porphyrin assemblies were destroyed in the presence of paraoxon, and QDs were isolated due to the formation of the associated systems between porphyrin molecules and paraoxon as illustrated in Scheme 1. The structures of TPyP and paraoxon are shown in Fig. S1 (see the ESI†). Pursuant to the literature binding interactions between porphyrins and aromatic ligands, notably purine and pyrimidine compounds,[30] occur through the attractive noncovalent process of π–π stacking, characteristic of a π-stacked complex formation.[31–34] Since porphyrin compounds possess an aromatic structure, and paraoxon has a phosphorus–oxygen double bond (P═O) and three oxygen atoms (Fig. S1, see the ESI†), the interactions between them result in the formation of π-stacked complexes. Both paraoxon and porphyrin possess an aromatic structure, therefore they are capable of forming stacked complexes,[35] as demonstrated in the interceptor molecule hypothesis postulated by Hartman and Shankel,[36] which explains the existence of stacking interactions between the interceptor (flat ring system) and the intercalator (polycyclic molecule). Moreover, paraoxon interacts with porphyrin by a hydrogen bond as well as interacts with an endocyclic nitrogen atom of a porphyrin cave. In addition to that, the fluorescence intensity of TPyP decreases with the increase of paraoxon concentration, as shown in Fig. S2 (see the ESI†). Fig. S2† shows a linear relationship between the concentration of paraoxon and the quenched fluorescence intensity of TPyP. The curvature was obtained, indicating the presence of a static quenching process, connected with the formation of ground state complexes with paraoxon, accompanied simultaneously by the additional specific binding interactions. We can obtain a linear relationship between the fluorescence intensity ratio I/I_0 (I and I_0 refer to the fluorescence intensity of TPyP in the presence and absence of paraoxon, respectively) and the concentration of paraoxon in the range of 9.09×10^{-8}–1.45×10^{-6} mol L^{-1}. When the paraoxon was detected only by a fluorescence change of the only porphyrin, the detection limit of this method was relatively low.

We recorded the fluorescence spectrum change of the QD/TPyP FRET system upon addition of various amounts of paraoxon at pH 8.5; and we also established a working curve from the fluorescence intensity ratio I_{TPyP}/I_{QDs} *versus* paraoxon concentration, as shown in Fig. 3 and 4. It was obvious that the presence of paraoxon significantly reduced the efficiency of the FRET system. As shown in Fig. 4, the correlation of paraoxon concentration with the fluorescence intensity ratio I_{TPyP}/I_{QDs} provided the basis for quantitative analysis, which resulted in a linear relationship within a range of 9.09×10^{-12}–1.09×10^{-6} mol L^{-1} paraoxon. The linear regression equation was $I_{TPyP}/I_{QDs} = -0.999–0.293 \log C_{paraoxon}$ (mol L^{-1}) with the correlation coefficient (R^2) of 0.999. The limit of detection

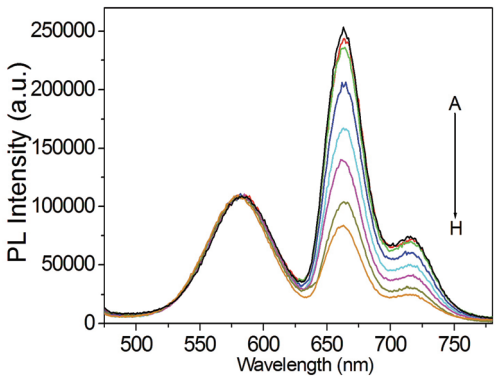

Fig. 3 Fluorescence spectra of TPyP in the presence of paraoxon at various concentrations. A–H represents the concentration of paraoxon of 0, 9.09×10^{-12}, 1.82×10^{-11}, 1.82×10^{-10}, 1.82×10^{-9}, 1.82×10^{-8}, 1.82×10^{-7} and 1.82×10^{-6} mol L^{-1}, respectively.

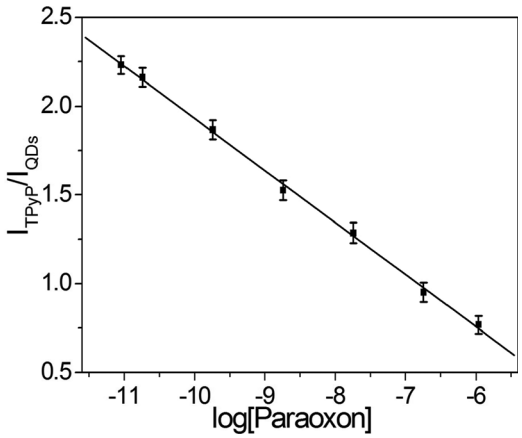

Fig. 4 The relationship between I_{TPyP}/I_{QDs} (I_{TPyP} and I_{QDs} refer to the fluorescence intensity of TPyP and CdTe QDs, respectively) and the concentration of paraoxon.

(LOD) corresponding to the fluorescence intensity 3 times the standard deviation obtained from 11 fluorescence measurements in the absence of analytes was 3.15×10^{-12} mol L^{-1}.

Interference study

Commonly existing foreign substances may affect the performance of the detection system in the real samples. To assess the precision of the proposed method, solutions containing different potential interferences were tested under the same conditions in the existing 1.82×10^{-10} mol L^{-1} paraoxon. Table 1 shows the interference effect of inorganic ions, sugar, organic acids, other aromatic compounds and OPs on the determination of paraoxon, and a relative error of ±5.0% was considered to be tolerable. As shown in Table 1, the results show that the tolerable concentration ratios of the coexisting substances to 1.82×10^{-10} mol L^{-1} paraoxon were over 10^8-fold for NaCl and KCl, 10^3-fold for $CaCl_2$, and $Mg(NO_3)_2$, 500-fold for $Zn(NO_3)_2$, $FeCl_3$, $MnSO_4$ and $CuSO_4$, 10^7-fold for glucose and glycine, 10^3-fold for vitamin C, 10^6-fold for 2-nitrophenol and phenol, and 500-fold for parathion. It was found that there was little interference from the commonly existing substances. Thus, the new sensitive method displayed high selectivity for the determination of paraoxon.

Table 1 The interference of coexisting substances in the determination of paraoxon (1.82×10^{-10} mol L^{-1})

Coexisting substance	Tolerable concentration (mol L^{-1})	Molar ratio	$\Delta I/I$ (%)
NaCl	1.82×10^{-2}	10^8	1.44
KCl	1.82×10^{-2}	10^8	−2.86
$CaCl_2$	1.82×10^{-6}	10^3	−1.24
$Mg(NO_3)_2$	1.82×10^{-6}	10^3	−2.80
$Zn(NO_3)_2$	9.10×10^{-8}	500	−1.75
$FeCl_3$	9.10×10^{-8}	500	−0.28
$MnSO_4$	9.10×10^{-8}	500	−4.42
$CuSO_4$	9.10×10^{-8}	500	2.55
Glucose	1.82×10^{-3}	10^7	2.86
Glycine	1.82×10^{-3}	10^7	−4.33
Vitamin C	1.82×10^{-6}	10^3	−1.75
2-nitrophenol	1.82×10^{-4}	10^6	2.06
Phenol	1.82×10^{-4}	10^6	2.67
Parathion	9.10×10^{-8}	500	2.29

$\Delta I = I_0 - I$, where I_0 and I are the fluorescence intensity ratios, I_{TPyP}/I_{QDs} *versus* in the absence and presence of interfering species.

Analysis of paraoxon in real samples

In order to demonstrate the practical applicability of this method, it was applied to detect the paraoxon in fruit samples. In conventional monitoring techniques, these compounds need to be extracted by organic media and concentrated afterwards, which are time- and cost-consuming and liable to pesticide loss. In the present work, the fruit samples were simply pretreated as described in the Experimental section without using organic solvents and tedious preconcentration steps. Further experiments were performed with the intentional addition of paraoxon onto the apple surface. As shown in Table 2, the testing recoveries are from 101% to 103%, and the RSDs were less than 2.0%. The results revealed that it was an applicable method for organophosphate compound-contaminated food samples. GC was performed as a comparative method. The recovery of paraoxon added to fruit samples is 110.2% at a concentration level of 7.27×10^{-7} mol L^{-1}, indicating an acceptable accuracy for the total OP content in the fruit samples with the proposed biosensor. Compared with the comparative data, the results were reliable and satisfactory.

Table 2 Determination of paraoxon in the fruit samples

Sample	Added (10^{-11} mol L^{-1})	Found[a] (10^{-11} mol L^{-1})	Recovery (%)	RSD (%, $n = 3$)
Apple	0.00	0.00	—	—
	9.09	9.21	101.3	0.9
	18.17	18.66	102.7	1.9

[a] Mean of three replicates.

Conclusion

In conclusion, a FRET system based on CdTe QDs and TPyP makes the detection method of OPs more sensitive, rapid, and selective. In the established FRET system, the addition of paraoxon inhibits the resonance energy transfer between CdTe QDs and TPyP, thus, resulting in the fluorescence decrease of TPyP. Under the optimized experimental conditions, paraoxon could be detected based on the fluorescence intensity ratio I_{TPyP}/I_{QDs} changes in the FRET system. The proposed method is applied to the determination of paraoxon in real samples with satisfactory results. On the basis of this designing strategy, it should be possible to develop a novel class of OP probes based on QDs and porphyrin.

Acknowledgements

This work was financially supported by a grant from the National Natural Science Foundation of China (no. 31501564, 31471639), a grant from the National Key Technologies R & D Program of China during the 12th Five-Year Plan Period (no. 2012BAD29B06), the Research Project from the Science & Technology Department of Liaoning Province of China (no. 2015103020), the Team Support Program for the Taishan Scholar of Blue Industry leading personnel of shandong Province of China (LZBZ2015-19), and the Open Foundation of Food Safety Key Laboratory of Liaoning Province (LNSAKF2013012).

References

1 X. J. Ji, J. Y. Zheng, J. M. Xu, V. K. Rastogi, T. C. Cheng, J. J. DeFrank and R. M. Leblanc, *J. Phys. Chem. B*, 2005, **109**, 3793–3799.
2 V. Vamvakaki and N. A. Chaniotakis, *Biosens. Bioelectron.*, 2007, **22**, 2848–2853.
3 P. S. Chen and S. D. Huang, *Talanta*, 2006, **69**, 669–675.
4 C. C. Leandro, P. Hancock, R. J. Fussell and B. J. Keely, *J. Chromatogr., A*, 2006, **1103**, 94–101.
5 Y. Zhao, Y. Ma, H. Li and L. Wang, *Anal. Chem.*, 2012, **84**, 386–395.
6 D. Du, J. Wang, L. Wang, D. Lu and Y. Lin, *Anal. Chem.*, 2012, **84**, 1380–1385.
7 X. X. Jiang, H. Y. Shi, N. Wu and M. H. Wang, *Food Chem.*, 2011, **125**, 1385–1389.
8 K. Zhang, Q. Mei, G. Guan, B. Liu, S. Wang and Z. Zhang, *Anal. Chem.*, 2010, **82**, 9579–9586.
9 S. H. Wang, M. Y. Han and D. J. Huang, *J. Am. Chem. Soc.*, 2009, **131**, 11692–11694.
10 G. W. Chen, F. L. Song, X. Q. Xiong and X. J. Peng, *Ind. Eng. Chem. Res.*, 2013, **52**, 11228–11245.
11 Q. J. Sun, Y. A. Wang, L. S. Li, D. Y. Wang, T. Zhu, J. Xu, C. H. Yang and Y. F. Li, *Nat. Photonics*, 2007, **1**, 717–722.
12 Q. J. Sun, S. Guru, L. M. Dai, C. Michael, C. Angela, N. Rajesh, G. James and Y. Q. Wang, *ACS Nano*, 2009, **3**, 737–743.
13 J. J. Guo, Y. Zhang, Y. L. Luo, F. Shen and C. Y. Sun, *Talanta*, 2014, **25**, 385–392.
14 M. Shalom, S. Dor, S. Ruhle, L. Grinis and A. Zaban, *J. Phys. Chem. C.*, 2009, **113**, 3895–3898.
15 D. Zhao, Y. Fan, F. Gao and T. M. Yang, *Anal. Chim. Acta*, 2015, **888**, 131–137.
16 P. M. Keane and J. M. Kelly, *Photochem. Photobiol. Sci.*, 2011, **10**, 1578–1586.
17 J. Zawacka-Pankau, J. Krachulec and I. Grulkowski, *Toxicol. Appl. Pharmacol.*, 2008, **232**, 487–497.
18 M. Makarska-Bialokoz, *Cent. Eur. J. Chem.*, 2013, **11**, 1360–1367.
19 M. Makarska-Bialokoz, *J. Lumin.*, 2014, **147**, 27–33.
20 B. J. Johnson, B. J. Melde, C. Thomas, A. P. Malanoski, I. A. Leska, P. T. Charles, D. A. Parrish and J. R. Deschamps, *Sensors*, 2010, **10**, 2315–2331.
21 R. Buntem, A. Intasiri and W. J. Lueangchaichaweng, *Colloids Interfaces Sci.*, 2010, **347**, 8–14.
22 F. Zhi, X. Lu, J. Yang, X. Wang, H. Shang, S. Zhang and Z. Xue, *J. Phys. Chem. C*, 2009, **113**, 13166–13172.
23 S. Mandal, M. Rahaman, S. Sadhu, S. K. Nayak and A. Patra, *J. Phys. Chem. C*, 2013, **117**, 3069–3077.
24 T. Blaudeck, E. I. Zenkevich, M. A. Mottaleb, K. Szwaykowska, D. Kowerko, F. Cichos and C. von Borczyskowski, *ChemPhysChem*, 2012, **13**, 959–972.
25 C. Wang, Q. Ma and X. G. Su, *J. Nanosci. Nanotechnol.*, 2008, **8**, 4408–4414.
26 *Chinese National Standards GB/T5009.199-2003*, Standards Press of China, Beijing, 2003.
27 C. M. Lemon, K. Elizabeth, M. G. Bawendi and D. G. Nocera, *Inorg. Chem.*, 2013, **52**, 10394–10406.
28 J. Li, F. Mei, W. Y. Li, X. W. He and Y. K. Zhang, *Spectrochim. Acta, Part A*, 2008, **70**, 811–817.
29 A. R. Clapp, I. L. Medintz and H. Mattoussi, *ChemPhysChem*, 2006, **7**, 47–57.
30 J. R. Lakowicz, *Principles of fluorescence spectroscopy*, Springer, 3rd edn, 2006.
31 A. Osowski, M. Pietrzak, Z. Wieczorek and J. Wieczorek, *J. Toxicol. Environ. Health, Part A*, 2010, **73**, 1141–1149.
32 I. V. Sazanovich, E. P. Petrov and V. S. Chirvony, *Opt. Spectrosc.*, 2006, **100**, 209–218.
33 P. M. Keane and J. M. Kelly, *Photochem. Photobiol. Sci.*, 2011, **10**, 1578–1586.
34 T. Yamashita, T. Uno and Y. Ishikawa, *Bioorg. Med. Chem.*, 2005, **13**, 2423–2430.
35 A. Osowski, M. Pietrzak, Z. Wieczorek and J. Wieczorek, *J. Toxicol. Environ. Health, Part A*, 2010, **73**, 1141–1149.
36 P. E. Hartman and D. M. Shankel, *Environ. Mol. Mutagen.*, 1990, **67**, 145–182.

